

Contents lists available at [SciVerse ScienceDirect](http://www.sciencedirect.com)

## Journal of Sound and Vibration

journal homepage: [www.elsevier.com/locate/jsvi](http://www.elsevier.com/locate/jsvi)

# Analytical solution for free vibrations of moderately thick hybrid piezoelectric laminated plates

M.A. Askari Farsangi<sup>a</sup>, A.R. Saidi<sup>a</sup>, R.C. Batra<sup>b,\*</sup><sup>a</sup> Department of Mechanical Engineering, Shahid Bahonar University of Kerman, Kerman, Iran<sup>b</sup> Department of Engineering Science and Mechanics, Virginia Polytechnic Institute and State University, Blacksburg, VA 24061, USA

## ARTICLE INFO

## Article history:

Received 2 January 2013

Received in revised form

13 May 2013

Accepted 14 May 2013

Handling Editor: S. Ilanko

Available online 12 July 2013

## ABSTRACT

An analytical solution for free vibrations of a hybrid rectangular plate composed of a transversely isotropic, homogeneous and linear elastic core and face sheets made of a linear piezoelectric material is derived by assuming that the plate deformations are governed by the Mindlin plate theory. The electric potential in a piezoelectric layer satisfies Maxwell's equation and either open circuit or closed circuit boundary conditions on its major surfaces. For the hybrid plate coupled governing equations obtained from the Hamilton principle are decoupled by introducing four auxiliary scalar functions, and the Levy type analytical solution for free vibrations is derived. Plate frequencies as a function of the piezoelectric layer thickness and the plate aspect ratio are presented and discussed. It is found that the electric boundary conditions on major surfaces of the piezoelectric layers and the aspect ratio of the hybrid plate noticeably influence its frequencies. Significant contributions of the work include proposing the four scalar functions to uncouple the governing equations, providing an analytical solution for frequencies of the hybrid plate, and delineating effects of boundary conditions as well as of aspect ratio of the plate.

© 2013 Elsevier Ltd. All rights reserved.

## 1. Introduction

Piezoelectric materials have wide ranging applications. Their electromechanical coupling characteristics, which lead to mechanical deformations under an electric field and electrical polarization under mechanical loads, make them suitable for a variety of electromechanical devices used for data collection [1], cooling systems [2], vibration and noise suppression [3], energy harvesting [4], and telecommunication and sensor networks [5].

Static and dynamic deformations of a single-layer piezoelectric plate have been analyzed by Tiersten [6]. Wang and Yang [7] have reviewed the development of higher order theories for dynamic analysis of piezoelectric plates and classified them according to the variation in the thickness direction of displacements and the electric potential. Batra and Vidoli [8] have proposed a  $K$ th order shear and normal deformable theory for piezoelectric plates in which both the electric potential and the three components of the mechanical displacement are expressed in terms of Legendre polynomials up to order  $K$  in the thickness coordinate. The governing equations have been derived by using a mixed variational principle and exactly satisfy electromechanical boundary conditions on the top and the bottom surfaces of the plate. Shiyekar and Kant [45] have used a higher-order shear and normal deformable plate theory to analyze deformations of a hybrid functionally graded laminate

\* Corresponding author. Tel.: +1 540 231 6051.

E-mail address: [rbatra@vt.edu](mailto:rbatra@vt.edu) (R.C. Batra).

with piezoelectric layers. Analytical results for free vibrations of piezoelectric plates are derived in Ref. [46], and the literature on smart structures has been reviewed by Chopra [47].

Numerous studies have been carried out on free vibrations of piezoelectric coupled laminated plates. Tzou and Tseng [9] proposed an integrated distributed piezoelectric sensor/actuator design for a large distributed system (shells and plates) and studied its dynamic characteristics. Heyliger et al. [10,24,25,35,36] have studied vibration problems for linear piezoelectric and linear magneto-electro-elastic laminates. Kapuria et al. [37,38] and Edery-Azulay and Abramovich [43] have proposed an extended Kantorovich method for analyzing vibrations of piezoelectric laminates and finding inter-laminar stresses. An exact three-dimensional (3D) analysis of simply supported piezoelectric coupled laminated plate was presented by Batra et al. [11] in which thin piezoelectric layers are modeled as membranes. Vel and Batra [39] have studied 3D free vibrations of hybrid piezoelectric laminates, and Yang and Batra [48] of thermo-piezoelectric plates. Reddy [12] derived equations for laminated composite plates with integrated sensors and actuators based on the classical and shear deformation plate theories. Vel et al. [13] extended the Stroh formalism to obtain an analytical solution for the steady state cylindrical bending vibration of a composite plate with either surface mounted or embedded piezoelectric patches. The cylindrical bending vibrations of a simply supported laminate with an embedded piezoelectric shear actuator have been investigated by Baillargeon and Vel [14]. Using the finite layer method, Akhras and Li [15] studied 3D deformations of simply supported rectangular plates.

Topdar et al. [16] employed the finite element method (FEM) to study free vibrations of a piezoelectric coupled laminated plate under various boundary conditions. Batra and Liang [40], and Batra and Geng [41] employed the FEM to delineate 3-D free and forced vibrations of hybrid piezoelectric laminates undergoing large or finite deformations.

The vibration analysis of simply supported hybrid piezoelectric laminated plates using the classical plate theory (CPT) and the first order shear deformation theory (FSDT or the Mindlin plate theory) was conducted by Pietrzakowski [17]. Free vibrations of simply supported orthotropic cross-ply laminates with piezoelectric layers bonded to the top and the bottom surfaces have been studied by Torres and Mendonça [18], and Jin and Batra [19]. Whereas Torres and Mendonça assumed mechanical displacements based on a higher order shear deformation theory, Jin and Batra used the FSDT; in both studies the electric potential had layer wise discretization in the thickness direction.

For a simply supported laminated plate with embedded piezoelectric layers, Liang and Batra [20] investigated effects of thickness, mass density and stiffness of the piezoelectric layer on plate's natural frequencies. The effect of electrical boundary conditions on major surfaces of piezoelectric layers was studied by Davis and Lesieutre [21]. Jin and Batra [19], and Wu et al. [22] have shown that natural frequencies for the closed circuit and the open circuit conditions are quite different. Kapuria et al. [42] have recently reviewed the literature on piezoelectric composite laminates. Benjeddou [44] has provided new insights into vibrations of piezoelectric beams.

Many studies on free vibrations of hybrid plates having layers made of piezoelectric and non-piezoelectric materials are based on the CPT [17,22]. As shown in [23] the CPT does not fully capture effects of the piezoelectric layer thickness on natural frequencies of the coupled structure. Works using either the FSDT or a higher-order plate theory have numerically analyzed frequencies of hybrid plates. Here we present an analytical solution for free vibrations of a transversely isotropic plate with two identical (i.e., the same thickness and the same material) piezoelectric layers bonded to its top and the bottom surfaces. Two opposite edges of the plate are assumed to be simply supported but the other two edges can have different boundary conditions. Similarly, the electric potential is taken to vanish at two opposite edges and the other two edges can have either vanishing electric potential or overall null electric displacement. Equations governing free vibrations of the plate are decoupled by introducing four auxiliary functions. The Levy type solution that identically satisfies boundary conditions on simply supported edges is used to derive differential equations and boundary conditions for the four auxiliary functions. Numerical results for natural frequencies of the hybrid plate are presented, and changes in frequencies of the core plate due to the addition of piezoelectric layers are identified. Furthermore, effects of open circuit versus closed circuit boundary conditions on major surfaces of the two piezoelectric layers are delineated.

Significant contributions of the work include using the FSDT theory for the hybrid plate and quadratic variation of the electric potential through the piezoelectric layer thickness, introducing four scalar functions to decouple the governing equations, analytically solving these equations, and delineating effects of closed and open circuit electric boundary conditions on the hybrid plate frequencies.

## 2. Problem formulation

A schematic sketch of the problem studied is depicted in Fig. 1. The plate has length  $a$ , width  $b$ , core thickness  $2h$  and thickness of each piezoelectric layer  $h_p$  with the mid-surface of the hybrid plate lying in the  $xy$ -plane. The piezoelectric and the core materials are assumed to be homogeneous and transversely isotropic with the  $z$ -axis as the axis of transverse isotropy, and obey linear relations for both mechanical and electromechanical deformations.

For the FSDT, we assume the following displacement field:

$$u_x(x, y, z, t) = u_0(x, y, t) + z\psi_x(x, y, t) \quad (1a)$$

$$u_y(x, y, z, t) = v_0(x, y, t) + z\psi_y(x, y, t) \quad (1b)$$

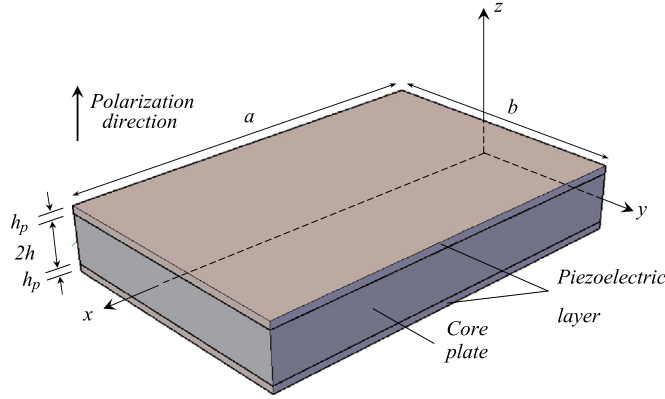


Fig. 1. Schematic sketch of the hybrid rectangular plate studied.

$$u_z(x, y, z, t) = w(x, y, t) \tag{1c}$$

in which,  $u_0$ ,  $v_0$ , and  $w$  are displacements along the  $x$ -, the  $y$ -, and the  $z$ -axis, respectively, of a point on the mid-surface, and  $\psi_x$  and  $\psi_y$  represent rotations about the  $y$ - and the  $x$ -axis, respectively. The assumed displacement field (1) gives continuous displacements across interfaces between the piezoelectric layers and the core plate.

In rectangular Cartesian coordinates, the strain–displacement relation for infinitesimal deformations is

$$\{\boldsymbol{\varepsilon}\} = \frac{1}{2}(\nabla \mathbf{u} + (\nabla \mathbf{u})^T) \tag{2}$$

where  $\nabla$  is the gradient operator. The linear constitutive relations for the elastic core and the piezoelectric layers are taken to be

$$\{\boldsymbol{\sigma}\} = [\mathbf{C}]\{\boldsymbol{\varepsilon}\} \tag{3}$$

$$\{\boldsymbol{\sigma}\} = [\mathbf{C}']\{\boldsymbol{\varepsilon}\} - [\mathbf{e}]^T \{\mathbf{E}\}, \quad \{\mathbf{D}\} = [\mathbf{e}]\{\boldsymbol{\varepsilon}\} + [\boldsymbol{\Xi}]\{\mathbf{E}\} \tag{4}$$

where  $\{\mathbf{E}\}$  and  $\{\mathbf{D}\}$  are the electric field and the electrical displacement in the piezoelectric layer, respectively,  $[\mathbf{C}]$  and  $[\mathbf{C}']$  are, respectively, matrices of elastic constants for the core and the piezoelectric layer,  $[\boldsymbol{\Xi}]$  is the matrix of dielectric permittivity, and  $[\mathbf{e}]$  is the electromechanical coupling matrix. These matrices, modified by solving the equation  $\sigma_{zz} = 0$  for  $\varepsilon_{zz}$  and substituting for  $\varepsilon_{zz}$  in Eqs. (3) and (4), are given as relations (A.1) in Appendix A. The electric potential  $\Phi$  is related to the electric field by

$$\mathbf{E} = -\nabla \Phi \tag{5}$$

Using Hamilton's principle, we get the following equations of motion [26]:

$$N_{xx,x} + N_{xy,y} = I_0 \ddot{u}_0, \quad N_{xy,x} + N_{yy,y} = I_0 \ddot{v}_0, \quad Q_{x,x} + Q_{y,y} = I_0 \ddot{w} \tag{6a}$$

$$M_{xx,x} + M_{xy,y} - Q_x = I_2 \ddot{\psi}_x, \quad M_{xy,x} + M_{yy,y} - Q_y = I_2 \ddot{\psi}_y \tag{6b}$$

In Eqs. (6a) and (6b) a superimposed dot denotes differentiation with respect to time  $t$ , and the in-plane resultant forces  $(N_{xx}, N_{xy}, N_{yy})$ , resultant moments  $(M_{xx}, M_{xy}, M_{yy})$ , the resultant transverse forces  $(Q_x, Q_y)$ , and the mass moments of inertia  $(I_0, I_2)$  are defined below:

$$\begin{aligned} (N_{xx}, N_{xy}, N_{yy}) &= \int_{-h-h_p}^{h+h_p} (\sigma_{xx}, \sigma_{xy}, \sigma_{yy}) dz, \quad (Q_x, Q_y) = \int_{-h-h_p}^{h+h_p} (\sigma_{xz}, \sigma_{yz}) dz \\ (M_{xx}, M_{xy}, M_{yy}) &= \int_{-h-h_p}^{h+h_p} (\sigma_{xx}, \sigma_{xy}, \sigma_{yy}) z dz, \quad (I_0, I_2) = \int_{-h-h_p}^{h+h_p} \rho(1, z^2) dz \end{aligned} \tag{7}$$

We neglect inertia effects for the electrical problem since time scales for it are much smaller than those for the mechanical problem. The continuity of surface tractions at the interfaces between the piezoelectric layers and the core plate has been tacitly assumed in deriving Eqs. (6). Analogous to Eqs. (6) for the mechanical equilibrium, we satisfy the Maxwell equation in the following integral form:

$$\int_h^{h+h_p} \nabla \cdot \mathbf{D} dz + \int_{-h-h_p}^{-h} \nabla \cdot \mathbf{D} dz = \int_h^{h+h_p} (D_{x,x} + D_{y,y} + D_{z,z}) dz + \int_{-h-h_p}^{-h} (D_{x,x} + D_{y,y} + D_{z,z}) dz = 0 \tag{8}$$

The top and the bottom surfaces of the hybrid laminate are traction free. We consider one of the following two electrical boundary conditions on major surfaces of the piezoelectric layers.

$$\Phi(z = \pm h) = 0, \quad \Phi(z = \pm (h + h_p)) = 0; \tag{9a}$$

$$\Phi(z = \pm h) = 0, \quad D_z(z = \pm (h + h_p)) = 0 \tag{9b}$$

That is, in each case the interface between the piezoelectric layer and the core plate is at zero potential, and the outermost surfaces of the piezoelectric layer are either held at zero potential or are electrically insulated. The edges  $x = 0$  and  $x = a$  are assumed to be at zero potential, and on the other two edges  $y = -b/2$  and  $y = b/2$  either the electric potential is prescribed to be zero or they are electrically insulated in which case the following boundary condition holds:

$$\int_h^{h+h_p} D_y\left(x, \pm \frac{b}{2}, z, t\right) dz + \int_{-h-h_p}^{-h} D_y\left(x, \pm \frac{b}{2}, z, t\right) dz = 0 \tag{10}$$

We consider the following mechanical boundary conditions on edges  $y = -b/2$  and  $y = b/2$ :

(i) Clamped:

$$u_0 = v_0 = w = \psi_x = \psi_y = 0 \tag{11a}$$

(ii) Free:

$$N_{xy} = N_{yy} = Q_y = M_{xy} = M_{yy} = 0 \tag{11b}$$

(iii) Simply supported:

$$N_{xy} = N_{yy} = w = M_{xy} = M_{yy} = 0 \tag{11c}$$

The other two edges,  $x = 0$  and  $x = a$ , are assumed to be simply supported with boundary conditions analogous to Eq. (11c) applied on them. Free, clamped and simply supported edges are denoted by F, C and S, respectively.

### 3. Analytical solution

#### 3.1. Electric problem

When the two major surfaces of the piezoelectric layer are held at zero voltage (i.e., closed circuit or boundary conditions (9a) prescribed on them), we assume the following quadratic variation of  $\Phi$  in the transverse coordinate,  $z$  [27]:

$$\Phi(x, y, z, t) = \begin{cases} \varphi(x, y, t) \left[ 1 - \left( \frac{z-h-h_p/2}{h_p/2} \right)^2 \right], & h \leq z \leq h + h_p \\ \varphi(x, y, t) \left[ 1 - \left( \frac{-z-h-h_p/2}{h_p/2} \right)^2 \right], & -h-h_p \leq z \leq -h \end{cases} \tag{12a}$$

However, when one surface is kept at zero voltage and the other is electrically insulated (i.e., open circuit or boundary conditions (9b) prescribed on them), we postulate that

$$\Phi(x, y, z, t) = \begin{cases} \varphi(x, y, t) \left[ 1 - \left( \frac{z-h-h_p/2}{h_p/2} \right)^2 + \frac{4(z-h)}{h_p} \right] + \frac{\bar{e}_{31}}{\bar{\epsilon}_{33}} [u_x + v_y + (h + h_p)(\psi_{x,x} + \psi_{y,y})](z-h) & h \leq z \leq h + h_p \\ \varphi(x, y, t) \left[ 1 - \left( \frac{-z-h-h_p/2}{h_p/2} \right)^2 + \frac{-4(z+h)}{h_p} \right] + \frac{\bar{e}_{31}}{\bar{\epsilon}_{33}} [u_x + v_y - (h + h_p)(\psi_{x,x} + \psi_{y,y})](z+h) & -h-h_p \leq z \leq -h \end{cases} \tag{12b}$$

with expressions for  $\bar{e}_{31}$  and  $\bar{\epsilon}_{33}$  given in Appendix A.

Substitution from Eq. (12) into Eq. (5) and the result into Eqs. (4) and (8) gives the following equation for the determination of the function  $\phi$  appearing in Eq. (12).

$$\mu_4(w_{,xx} + w_{,yy}) - \mu_2(\psi_{x,xxx} + \psi_{x,xyy} + \psi_{y,yxx} + \psi_{y,yyy}) - \mu_3(\phi_{,xx} + \phi_{,yy}) + \mu_5(\psi_{x,x} + \psi_{y,y}) + \mu_6\phi = 0 \tag{13}$$

Boundary conditions for  $\phi$  are

$$\begin{aligned} &\phi(a, y, t) = \phi(0, y, t) = 0, \text{ and} \\ &\text{either } \phi\left(x, \frac{b}{2}, t\right) = \phi\left(x, -\frac{b}{2}, t\right) = 0 \\ &\text{or } \int_h^{h+h_p} D_y\left(x, \pm \frac{b}{2}, z, t\right) dz + \int_{-h-h_p}^{-h} D_y\left(x, \pm \frac{b}{2}, z, t\right) dz = 0 \end{aligned} \tag{14}$$

Eq. (13) exhibits coupling between electrical and mechanical effects. For the open and the closed circuit conditions, material moduli  $\mu_2, \dots, \mu_6$  listed in Appendix A have different values.

### 3.2. Mechanical problem

Upon substitution of relations (1), (2), (3) and (4) into (7), resultant forces and resultant moments are expressed in terms of the generalized displacements and the electric potential  $\phi$  as

$$N_{xx} = A'_{11}u_{0,x} + A'_{12}v_{0,y}, \quad N_{yy} = A'_{12}u_{0,x} + A'_{11}v_{0,y}, \quad N_{xy} = A'_{66}(u_{0,y} + v_{0,x}) \quad (15a,b,c)$$

$$M_{xx} = D'_{11}\psi_{x,x} + D'_{12}\psi_{y,y} + \mu_1\phi, \quad M_{yy} = D'_{12}\psi_{x,x} + D'_{11}\psi_{y,y} + \mu_1\phi, \quad M_{xy} = D'_{66}(\psi_{x,y} + \psi_{y,x}) \quad (15d,e,f)$$

$$Q_x = K^2A'_{55}(w_x + \psi_x) - \mu_2(\psi_{x,xx} + \psi_{y,xy}) - \mu_3\phi_x \quad (15g)$$

$$Q_y = K^2A'_{55}(w_y + \psi_y) - \mu_2(\psi_{x,xy} + \psi_{y,yy}) - \mu_3\phi_y \quad (15h)$$

where  $K^2$  is the shear correction factor which is assumed to be  $\pi^2/12$ . Expressions for coefficients in relations (15a–h) are given as Eq. (A.2) of Appendix A.

Substitution from relations (15) into Eqs. (6) gives following equations for the displacements:

$$A'_{11}u_{0,xx} + A'_{12}v_{0,xy} + A'_{12}(u_{0,xx} + v_{0,xy}) = I_0\ddot{u}_0, \quad A'_{12}u_{0,xy} + A'_{11}v_{0,yy} + A'_{66}(u_{0,xy} + v_{0,xx}) = I_0\ddot{v}_0 \quad (16a,b)$$

$$D'_{11}\psi_{x,xx} + D'_{12}\psi_{y,xy} + D'_{66}(\psi_{x,yy} + \psi_{y,xy}) + \mu_2(\psi_{x,xx} + \psi_{y,xy}) - K^2A'_{55}(w_x + \psi_x) + (\mu_1 + \mu_3)\phi_x = I_2\ddot{\psi}_x \quad (16c)$$

$$D'_{12}\psi_{x,xy} + D'_{11}\psi_{y,yy} + D'_{66}(\psi_{x,xy} + \psi_{y,xx}) + \mu_2(\psi_{x,xy} + \psi_{y,yy}) - K^2A'_{55}(w_y + \psi_y) + (\mu_1 + \mu_3)\phi_y = I_2\ddot{\psi}_y \quad (16d)$$

$$K^2A'_{55}(w_{xx} + w_{yy} + \psi_{x,x} + \psi_{y,y}) - \mu_2(\psi_{x,xxx} + \psi_{x,xyy} + \psi_{y,yxx} + \psi_{y,yyy}) - \mu_3(\phi_{xx} + \phi_{yy}) = I_0\ddot{w} \quad (16e)$$

Eqs. (16a) and (16b) govern stretching ( $u_0$  and  $v_0$ ) of the plate midsurface, Eqs. (16c)–(16e) its bending ( $w$ ,  $\psi_x$ ,  $\psi_y$ ), and there is no coupling between the two types of deformations. However, Eqs. (16a) and (16b) are coupled, and so are Eqs. (16c)–(16e) and (13). We simplify these equations as follows.

We introduce four auxiliary functions  $\varphi_1$ ,  $\varphi_2$ ,  $\varphi_3$  and  $\varphi_4$  defined by

$$\begin{Bmatrix} \varphi_1 \\ \varphi_2 \\ \varphi_3 \\ \varphi_4 \end{Bmatrix} = \begin{Bmatrix} u_{0,x} + v_{0,y} \\ u_{0,y} - v_{0,x} \\ \psi_{x,x} + \psi_{y,y} \\ \psi_{x,y} - \psi_{y,x} \end{Bmatrix} \quad (17)$$

and rewrite Eqs. (16) and (13) as

$$A'_{11}\varphi_{1,x} + A'_{66}\varphi_{2,y} = I_0\ddot{u}_0, \quad A'_{11}\varphi_{1,y} - A'_{66}\varphi_{2,x} = I_0\ddot{v}_0 \quad (18a,b)$$

$$D'_{11}\varphi_{3,x} + D'_{66}\varphi_{4,y} - K^2A'_{55}(w_x + \psi_x) + \mu_2\varphi_{3,x} + (\mu_1 + \mu_3)\phi_x = I_2\ddot{\psi}_x \quad (18c)$$

$$D'_{11}\varphi_{3,y} - D'_{66}\varphi_{4,x} - K^2A'_{55}(w_y + \psi_y) + \mu_2\varphi_{3,y} + (\mu_1 + \mu_3)\phi_y = I_2\ddot{\psi}_y \quad (18d)$$

$$K^2A'_{55}(\nabla^2w + \varphi_3) - \mu_2\nabla^2\varphi_3 - \mu_3\nabla^2\phi = I_0\ddot{w}, \quad \mu_4\nabla^2w - \mu_2\nabla^2\varphi_3 - \mu_3\nabla^2\phi + \mu_5\varphi_3 + \mu_6\phi = 0 \quad (18e,f)$$

where  $\nabla^2$  is the 2D Laplace operator in the  $xy$ -plane. Differentiation of Eqs. (18a) and (18c) with respect to  $x$  and of Eqs. (18b) and (18d) with respect to  $y$ , and adding Eq. (18a) to Eq. (18b) and Eq. (18c) to Eq. (18d) give

$$A'_{11}\nabla^2\varphi_1 = I_0\ddot{\varphi}_1, \quad D'_{11}\nabla^2\varphi_3 - K^2A'_{55}(\nabla^2w + \varphi_3) + \mu_2\nabla^2\varphi_3 + (\mu_1 + \mu_3)\nabla^2\phi = I_2\ddot{\varphi}_3 \quad (19a,b)$$

Differentiation of Eqs. (18a) and (18c) with respect to  $y$  and of Eqs. (18b) and (18d) with respect to  $x$ , and subtracting Eq. (18a) from Eq. (18b) and Eq. (18c) from Eq. (18d) give

$$A'_{66}\nabla^2\varphi_2 = I_0\ddot{\varphi}_2, \quad D'_{66}\nabla^2\varphi_4 - K^2A'_{55}\varphi_4 = I_2\ddot{\varphi}_4 \quad (20a,b)$$

It can be seen that Eqs. (18a) through (18d) are replaced by four Eqs. (19) and (20). Whereas Eqs. (19a), (20a) and (20b) are uncoupled, Eqs. (19b), (18e) and (18f) are coupled. These six equations are solved for the six unknown functions  $\phi$ ,  $\varphi_1$ ,  $\varphi_2$ ,  $\varphi_3$ ,  $\varphi_4$  and  $w$ .

For harmonic motion the six unknowns  $\phi$ ,  $\varphi_1$ ,  $\varphi_2$ ,  $\varphi_3$ ,  $\varphi_4$  and  $w$  are assumed to have the following form:

$$w(x, y, t) = \sum_{m=1}^{\infty} w_m(x, y)e^{i\omega_m t}, \quad \phi(x, y, t) = \sum_{m=1}^{\infty} \phi_m(x, y)e^{i\omega_m t}$$

$$\varphi_1(x, y, t) = \sum_{m=1}^{\infty} \varphi_{1m}(x, y)e^{i\omega_m t}, \quad \varphi_2(x, y, t) = \sum_{m=1}^{\infty} \varphi_{2m}(x, y)e^{i\omega_m t}$$

$$\varphi_3(x, y, t) = \sum_{m=1}^{\infty} \varphi_{3m}(x, y) e^{i\omega_m t}, \quad \varphi_4(x, y, t) = \sum_{m=1}^{\infty} \varphi_{4m}(x, y) e^{i\omega_m t} \quad (21)$$

where  $\omega_m$  is a natural frequency of the plate.

Substituting from Eq. (21) into Eq. (18e,f) and (19b) and after algebraic manipulations we obtain the following three uncoupled differential equations with constant coefficients:

$$\lambda_1 \nabla^6 w_m + \lambda_2 \nabla^4 w_m + \lambda_3 \nabla^2 w_m + \lambda_4 w_m = 0, \quad \varphi_{3m} = \lambda'_1 \nabla^4 w_m + \lambda'_2 \nabla^2 w_m + \lambda'_3 w_m, \quad (22a,b)$$

$$\phi_m = \lambda''_1 \nabla^2 w_m + \lambda''_3 w_m + \lambda''_3 \varphi_{3m} \quad (22c)$$

Coefficients  $\lambda_i (i = 1, \dots, 4)$  and  $\lambda'_k, \lambda''_k (k = 1, 2, 3)$  with values depending upon  $h_p$  and  $h$  are given as relations (A.3) in Appendix A. They couple electrical and mechanical effects. Furthermore, substitution from Eq. (21) into Eqs. (19a) and (20) yields

$$A'_{11} \nabla^2 \varphi_{1m} = -I_0 \omega^2 \varphi_{1m}, \quad A'_{66} \nabla^2 \varphi_{2m} = -I_0 \omega^2 \varphi_{2m}, \quad D'_{66} \nabla^2 \varphi_{4m} - K^2 A'_{55} \varphi_{4m} = -I_2 \omega^2 \varphi_{4m} \quad (23a,b,c)$$

Eqs. (22) and (23) are coupled because coefficients are functions of the frequency  $\omega$ .

For a harmonic motion, displacements  $u_0, v_0, \psi_x$  and  $\psi_y$  are written as

$$\begin{aligned} u_0(x, y, t) &= \sum_{m=1}^{\infty} u_{0m}(x, y) e^{i\omega_m t}, & v_0(x, y, t) &= \sum_{m=1}^{\infty} v_{0m}(x, y) e^{i\omega_m t} \\ \psi_x(x, y, t) &= \sum_{m=1}^{\infty} \psi_{xm}(x, y) e^{i\omega_m t}, & \psi_y(x, y, t) &= \sum_{m=1}^{\infty} \psi_{ym}(x, y) e^{i\omega_m t} \end{aligned} \quad (24)$$

Substituting from Eqs. (21) and (24) into Eqs. (18a)–(18d), we get

$$u_{0m} = -\frac{1}{I_0 \omega^2} (A'_{11} \varphi_{1m,x} + A'_{66} \varphi_{2m,y}), \quad v_{0m} = -\frac{1}{I_0 \omega^2} (A'_{11} \varphi_{1m,y} - A'_{66} \varphi_{2m,x}) \quad (25a,b)$$

$$\psi_{xm} = -\frac{1}{I_2 \omega^2} [D'_{11} \varphi_{3m,x} + D'_{66} \varphi_{4m,y} - K^2 A'_{55} (w_{m,x} + \psi_{xm}) + \mu_2 \varphi_{3m,x} + (\mu_1 + \mu_3) \phi_{m,x}] \quad (25c)$$

$$\psi_{ym} = -\frac{1}{I_2 \omega^2} [D'_{11} \varphi_{3m,y} - D'_{66} \varphi_{4m,x} - K^2 A'_{55} (w_{m,y} + \psi_{ym}) + \mu_2 \varphi_{3m,y} + (\mu_1 + \mu_3) \phi_{m,y}] \quad (25d)$$

Thus generalized displacements and the electric potential can be found once we know  $\phi, \varphi_1, \varphi_2, \varphi_3, \varphi_4$  and  $w$ .

### 3.3. Analytical solution

Recalling that edges  $x=0$  and  $x=a$  are simply supported, we assume the following expressions for the transverse displacement  $w_m$  and functions  $\varphi_{1m}, \varphi_{2m}$  and  $\varphi_{4m}$ :

$$w_m(x, y) = \sum_{j=1}^{\infty} w_{mj}(y) \sin(\beta_j x), \quad \varphi_{1m}(x, y) = \sum_{j=1}^{\infty} \varphi_{1mj}(y) \sin(\beta_j x) \quad (26a,b)$$

$$\varphi_{2m}(x, y) = \sum_{j=1}^{\infty} \varphi_{2mj}(y) \cos(\beta_j x), \quad \varphi_{4m}(x, y) = \sum_{j=1}^{\infty} \varphi_{4mj}(y) \cos(\beta_j x) \quad (26c,d)$$

where  $\beta_j = j\pi/a$ . Substitution from Eqs. (26) into Eqs. (22a) and (23) results in four ordinary differential equations whose solutions are [29]

$$w_{mj}(y) = C_1 \sinh(\eta_1 y) + C_2 \cosh(\eta_1 y) + C_3 \sinh(\eta_2 y) + C_4 \cosh(\eta_2 y) + C_5 \sinh(\eta_3 y) + C_6 \cosh(\eta_3 y) \quad (27a)$$

$$\varphi_{1mj}(y) = C_7 \sinh(\eta_4 y) + C_8 \cosh(\eta_4 y) \quad (27b)$$

$$\varphi_{2mj}(y) = C_9 \sinh(\eta_5 y) + C_{10} \cosh(\eta_5 y) \quad (27c)$$

$$\varphi_{4mj}(y) = C_{11} \sinh(\eta_6 y) + C_{12} \cosh(\eta_6 y) \quad (27d)$$

in which  $C_k (k = 1, \dots, 12)$  are twelve unknown constants to be determined from twelve boundary conditions, six (5 listed in Eq. (11) and 1 for  $\phi$ ) at each edge,  $y = \pm b/2$ . Substitution from Eq. (27a) into Eq. (22a), we find that parameters  $\eta_k = \sqrt{\epsilon_k}$  ( $k = 1, 2, 3$ ) are roots of the following cubic equation:

$$\lambda_1 \epsilon^3 + (\lambda_2 - 3\beta_j^2 \lambda_1) \epsilon^2 + (\lambda_3 - 2\lambda_2 \beta_j^2 + 3\lambda_1 \beta_j^4) \epsilon + (\lambda_4 - \lambda_3 \beta_j^2 + \lambda_2 \beta_j^4 - \lambda_1 \beta_j^6) = 0 \quad (28)$$

Values of parameters  $\eta_4, \eta_5$  and  $\eta_6$  are obtained from relations (A.4) of Appendix A. Note that solutions (27) are valid for real values of  $\eta_k$ . For imaginary values of  $\eta_k$ , sinh and cosh become sin and cos, respectively. After having found  $w$  we get  $\varphi_{3m}$  from Eq. (22b) and then  $\phi$  from Eq. (22c). Eq (25) can now be used to ascertain the generalized displacements.

By imposing electrical and mechanical boundary conditions on edges  $y = -b/2$  and  $y = b/2$ , a system of twelve homogeneous linear algebraic equations is obtained. Setting the determinant of the coefficient matrix equal to zero, we obtain an algebraic equation for the determination of natural frequencies of the hybrid plate.

#### 4. Numerical results and discussion

Unless otherwise mentioned, numerical results for free vibrations of a hybrid rectangular plate with core made of  $Al_2O_3$  and piezoelectric layers of  $PZT-4$  are presented for various values of geometric parameters and different boundary conditions on edges  $y = \pm b/2$ . Values of material parameters are listed in Table 1. The notation SCSF for mechanical boundary conditions implies that edges  $x = 0$  and  $x = a$  are simply supported, and edges  $y = b/2$  and  $y = -b/2$  are clamped

**Table 1**  
Values of material parameters.

Property	Core plate		Piezoelectric layer			
	Ti-6Al-4V	$Al_2O_3$	G-1195 N	PZT-4	PZT-6B	BaTiO <sub>3</sub>
$E$ (GPa)	105.7	–	63.0	–	–	–
$\nu$	0.2981	–	0.3	–	–	–
$c_{11}$ (GPa)	–	460.2	–	132	168	150
$c_{12}$ (GPa)	–	174.7	–	71	84.7	65.3
$c_{33}$ (GPa)	–	509.5	–	115	163	146
$c_{13}$ (GPa)	–	127.4	–	73	84.2	66.2
$c_{55}$ (GPa)	–	126.9	–	26	35.5	43.9
$e_{31}$ (cm <sup>-2</sup> )	–	–	44.37	-4.1	-0.9	-4.3
$e_{33}$ (cm <sup>-2</sup> )	–	–	50.18	14.1	7.1	17.5
$e_{15}$ (cm <sup>-2</sup> )	–	–	14.13	10.5	4.6	11.4
$\Xi_{11}$ (nF m <sup>-1</sup> )	–	–	15.30	7.124	3.60	9.87
$\Xi_{33}$ (nF m <sup>-1</sup> )	–	–	15.00	5.841	3.42	11.16
$\rho$ (kg m <sup>-3</sup> )	4429	4000	7600	7500	7550	5700

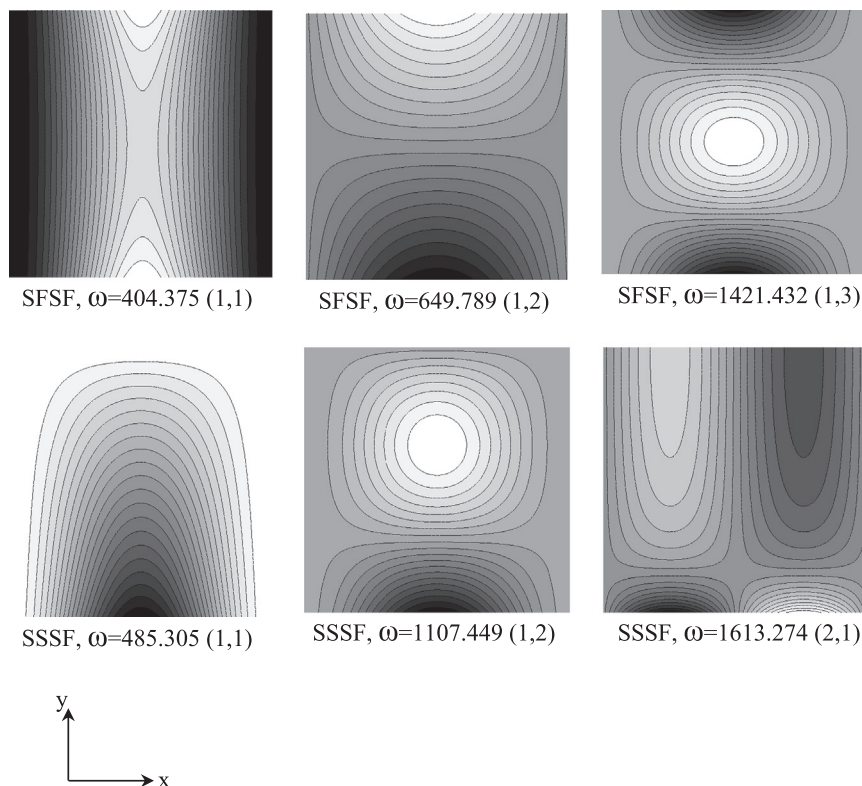


**Fig. 2.** Contour plots of the first three mode shapes for closed circuit piezoelectric coupled rectangular plate ( $b/a = 1$ ,  $2h/a = 0.1$ ,  $h_p/2h = 0.1$ ); the legends below each figure are boundary conditions, frequency (Hz), and the corresponding mode shape in  $x$ - and  $y$ -directions.

and free, respectively. Also, numbers in parenthesis following the value of the natural frequency equal the mode numbers along the  $x$  and the  $y$  directions, respectively. Contour plots of the first three mode shapes are exhibited in Fig. 2 for a hybrid piezoelectric rectangular plate under different mechanical boundary conditions.

4.1. Comparison of presently computed results with those in the literature

For a hybrid plate having an isotropic core, we have compared in Table 2 the presently computed resonant frequencies with those reported by Leissa [31] and Hasani et al. [32] for the thickness ratio  $h_p/2h$  decreasing from 0.1 to 0. It is clear that as  $h_p/2h$  goes to 0, the resonant frequency of the hybrid plate approaches that of the homogeneous plate. In Table 3 we have compared the first five natural frequencies of a SSSS square plate ( $2h/a=1/10$  and  $1/50$ ) made of a transversely isotropic material without piezoelectric layers with those reported in Ref. [28] based on the FSDT. It is clear that the presently

Table 2

Comparison of the non-dimensional natural frequency,  $\bar{\omega} = \omega a^2 \sqrt{12\rho(1-\nu^2)/E(2h)^2}$ , with that reported in Refs. [31,32] for different boundary conditions ( $b/a=1$  ;  $2h/a=0.005$ ).

$\frac{h_p}{2h}$	Reference	SSSS	SSSC	SSSF	SCSC	SCSF	SFSF
$10^{-1}$	Present	19.072	21.489	10.623	26.306	11.534	9.398
$10^{-2}$	Present	19.607	23.287	11.505	28.508	12.491	9.485
$10^{-4}$	Present	19.736	23.639	11.678	28.939	12.679	9.628
0	Present	19.738	23.643	11.680	28.944	12.681	9.630
0	Leissa [31]	19.74	23.65	11.680	28.95	12.69	9.63
0	Hasani et al. [32]	19.76	23.66	11.70	29.01	12.69	9.64

Table 3

Comparison of the non-dimensional natural frequency,  $\bar{\omega} = (a^2/2h)\omega\sqrt{\rho/G}$ , with that reported in reference [28] ( $a/b=1$  ;  $2h/a=1/50$  ,  $1/10$ ).

$\frac{2h}{a}$	Method	Mode number				
		1st	2nd	3rd	4th	5th
1/50	Present	9.6016	23.8922	23.8922	38.0519	47.4202
	Hosseini Hashemi et al.[28]	9.6016	23.8923	23.8923	38.0518	47.4200
1/10	Present	8.9605	20.4746	20.4746	30.3950	36.3614
	Hosseini Hashemi et al.[28]	8.9605	20.4745	20.4745	30.3949	36.3613

Table 4

Comparison of the non-dimensional natural frequency,  $\bar{\omega} = 2h\omega\sqrt{2\rho(1+\nu)/E}$ , with that reported in Ref. [33] ( $a/b=2$  ;  $2h/a=1/20$  ,  $1/12$ ).

Method	Mode number				
	(1,1)	(2,1)	(3,1)	(4,1)	(5,1)
$a/b=2, 2h/a=1/20$					
Present	0.0589	0.0930	0.1481	0.2218	0.3114
Srinivas et al. [33]	0.0589	0.0931	0.1485	0.2226	0.3130
$a/b=2, 2h/a=1/12$					
Present	0.1576	0.2444	0.3788	0.5497	-
Srinivas et al. [33]	0.1581	0.2455	0.3811	0.5544	-

Table 5

Comparison of the presently computed first ten natural frequencies (Hz) for an isotropic plate with those given in Ref. [30].

Method	Mode number									
	1st	2nd	3rd	4th	5th	6th	7th	8th	9th	10th
Present	145.35	363.05	363.05	580.35	725.00	725.00	941.64	941.64	1229.88	1229.88
He et al.[30]	144.25	359.00	359.00	564.10	717.80	717.80	908.25	908.255	1223.14	1223.14
Diff (%)	0.76	1.12	1.12	2.80	0.99	0.99	3.55	3.55	0.55	0.55

**Table 6**

The first three natural frequencies (Hz) for SSSS, SCSC, SFSF, SFSC, SSSC and SSSF hybrid plates with  $b/a = 1, 2$ ;  $2h/a = 0.05, 1$  and open and closed circuit conditions on major surfaces of the piezoelectric layers.

BCs.	$\frac{b}{a}$	$\frac{2h}{a}$	$\frac{h_p}{2h}$	Electrical condition	Mode sequences			
					1st	2nd	3rd	
SSSS	1	0.05	0.1	Closed	422.966 (1,1)	1038.436 (1,2)	1633.073 (2,2)	
				Open	429.818 (1,1)	1054.813 (1,2)	1658.196 (2,2)	
			0.2	Closed	405.858 (1,1)	992.919 (1,2)	1556.567 (2,2)	
		0.1	0.1	Open	418.993 (1,1)	1024.066 (1,2)	1604.047 (2,2)	
				Closed	816.534 (1,1)	1918.659 (1,2)	2910.463 (2,2)	
			0.2	Open	829.094 (1,1)	1945.644 (1,2)	2948.553 (2,2)	
	2	0.05	0.1	Closed	778.274 (1,1)	1810.841 (1,2)	2727.761 (2,2)	
				Open	802.005 (1,1)	1860.773 (1,2)	2797.491 (2,2)	
			0.2	Closed	265.592 (1,1)	422.966 (1,2)	682.077 (1,3)	
		0.1	0.1	Open	269.925 (1,1)	429.818 (1,2)	693.003 (1,3)	
				0.2	Closed	255.093 (1,1)	405.859 (1,2)	653.493 (1,3)
			Open	263.416 (1,1)	418.994 (1,2)	674.366 (1,3)		
	SCSC	1	0.05	0.1	Closed	519.218 (1,1)	816.537 (1,2)	1291.421 (1,3)
					Open	527.409 (1,1)	829.098 (1,2)	1310.531 (1,3)
				0.2	Closed	496.460 (1,1)	778.283 (1,2)	1225.300 (1,3)
			0.1	0.1	Open	512.042 (1,1)	802.024 (1,2)	1261.086 (1,3)
					0.2	Closed	609.652 (1,1)	1139.314 (2,1)
				Open	619.187 (1,1)	1156.901 (2,1)	1436.811 (1,2)	
2		0.05	0.1	Closed	583.692 (1,1)	1087.968 (2,1)	1348.827 (1,2)	
				Open	601.821 (1,1)	1121.272 (2,1)	1388.307 (1,2)	
			0.2	Closed	1128.191 (1,1)	2060.096 (2,1)	2456.099 (1,2)	
		0.1	0.1	Open	1143.582 (1,1)	2087.428 (2,1)	2484.766 (1,2)	
				0.2	Closed	1068.626 (1,1)	1939.224 (2,1)	2299.904 (1,2)
			Open	1097.013 (1,1)	1989.419 (2,1)	2351.255 (1,2)		
SFSF	1	0.05	0.1	Closed	293.724 (1,1)	503.042 (1,2)	814.007 (1,3)	
				Open	298.486 (1,1)	511.075 (1,2)	826.770 (1,3)	
			0.2	Closed	281.998 (1,1)	482.235 (1,2)	778.811 (1,3)	
		0.1	0.1	Open	291.132 (1,1)	497.582 (1,2)	803.077 (1,3)	
				0.2	Closed	569.657 (1,1)	953.729 (1,2)	1502.638 (1,3)
			Open	578.451 (1,1)	967.687 (1,2)	1523.345 (1,3)		
	2	0.05	0.1	Closed	543.984 (1,1)	906.499 (1,2)	1420.541 (1,3)	
				Open	560.636 (1,1)	932.611 (1,2)	1458.791 (1,3)	
			0.2	Closed	206.189 (1,1)	337.986 (1,2)	763.342 (1,3)	
		0.1	0.1	Open	208.514 (1,1)	339.685 (1,2)	771.475 (1,3)	
				0.2	Closed	198.324 (1,1)	325.041 (1,2)	730.608 (1,3)
			Open	202.751 (1,1)	328.241 (1,2)	746.136 (1,3)		
SFSC	1	0.05	0.1	Closed	404.375 (1,1)	649.789 (1,2)	1421.432 (1,3)	
				Open	408.708 (1,1)	652.670 (1,2)	1435.764 (1,3)	
			0.2	Closed	387.512 (1,1)	620.529 (1,2)	1341.602 (1,3)	
		0.1	0.1	Open	395.673 (1,1)	625.835 (1,2)	1368.417 (1,3)	
				0.2	Closed	209.027 (1,1)	248.830 (1,2)	374.330 (1,3)
			Open	211.803 (1,1)	251.256 (1,2)	378.263 (1,3)		
	2	0.05	0.1	Closed	200.962 (1,1)	239.324 (1,2)	359.581 (1,3)	
				Open	206.264 (1,1)	243.933 (1,2)	367.098 (1,3)	
			0.2	Closed	410.083 (1,1)	485.305 (1,2)	721.037 (1,3)	
		0.1	0.1	Open	415.302 (1,1)	489.721 (1,2)	728.174 (1,3)	
				0.2	Closed	392.803 (1,1)	464.619 (1,2)	687.823 (1,3)
			Open	402.675 (1,1)	472.893 (1,2)	701.266 (1,3)		
SSSC	1	0.05	0.1	Closed	268.928 (1,1)	690.400 (1,2)	874.395 (2,1)	
				Open	271.272 (1,1)	699.012 (1,2)	884.795 (2,1)	
			0.2	Closed	258.617 (1,1)	660.946 (1,2)	837.299 (2,1)	
		0.1	0.1	Open	263.059 (1,1)	677.343 (1,2)	856.916 (2,1)	
				0.2	Closed	521.069 (1,1)	1279.972 (1,2)	1626.329 (2,1)
			Open	525.238 (1,1)	1294.296 (1,2)	1643.159 (2,1)		
	2	0.05	0.1	Closed	498.408 (1,1)	1210.157 (1,2)	1538.612 (2,1)	
				Open	506.178 (1,1)	1236.695 (1,2)	1569.413 (2,1)	
			0.2	Closed	223.354 (1,1)	335.483 (1,2)	545.498 (1,3)	
		0.1	0.1	Open	226.144 (1,1)	339.790 (1,2)	553.021 (1,3)	
				0.2	Closed	214.743 (1,1)	322.211 (1,2)	522.984 (1,3)
			Open	220.065 (1,1)	330.453 (1,2)	537.360 (1,3)		
SSSF	0.05	0.1	Closed	437.198 (1,1)	647.963 (1,2)	1033.508 (1,3)		
			Open	442.398 (1,1)	655.808 (1,2)	1046.700 (1,3)		
		0.2	Closed	418.649 (1,1)	618.485 (1,2)	981.599 (1,3)		
	0.1	0.1	Open	428.458 (1,1)	633.282 (1,2)	1006.306 (1,3)		
			0.2	Closed	503.042 (1,1)	1082.550 (2,1)	1217.137 (1,2)	
		Open	511.074 (1,1)	1099.479 (2,1)	1235.814 (1,2)			

Table 6 (continued)

BCs.	$\frac{b}{a}$	$\frac{2h}{a}$	$\frac{h_p}{2h}$	Electrical condition	Mode sequences		
					1st	2nd	3rd
SSSF	2	0.2	0.2	Closed	482.234 (1,1)	1034.542 (2,1)	1161.780 (1,2)
				Open	497.579 (1,1)	1066.688 (2,1)	1197.091 (1,2)
			0.1	Closed	953.725 (1,1)	1982.268 (2,1)	2181.779 (1,2)
				Open	967.680 (1,1)	2009.514 (2,1)	2209.926 (1,2)
			0.2	Closed	906.485 (1,1)	1868.745 (2,1)	2051.053 (1,2)
				Open	932.582 (1,1)	1919.065 (2,1)	2102.378 (1,2)
		0.05	0.1	Closed	277.770 (1,1)	459.928 (1,2)	744.988 (1,3)
				Open	282.290 (1,1)	467.332 (1,2)	756.803 (1,3)
			0.2	Closed	266.745 (1,1)	441.134 (1,2)	713.296 (1,3)
				Open	275.423 (1,1)	455.305 (1,2)	735.818 (1,3)
			0.1	Closed	541.275 (1,1)	880.650 (1,2)	1393.625 (1,3)
				Open	549.739 (1,1)	893.898 (1,2)	1413.568 (1,3)
	1	0.2	Closed	517.271 (1,1)	838.300 (1,2)	1319.938 (1,3)	
			Open	533.344 (1,1)	863.223 (1,2)	1357.043 (1,3)	
		0.1	Closed	248.830 (1,1)	584.511 (1,2)	865.376 (2,1)	
			Open	251.256 (1,1)	591.647 (1,2)	875.988 (2,1)	
		0.2	Closed	239.324 (1,1)	560.378 (1,2)	828.724 (2,1)	
			Open	243.932 (1,1)	574.021 (1,2)	848.760 (2,1)	
	2	0.1	Closed	485.305 (1,1)	1107.449 (1,2)	1613.274 (2,1)	
			Open	489.720 (1,1)	1120.164 (1,2)	1630.546 (2,1)	
		0.2	Closed	464.618 (1,1)	1050.948 (1,2)	1526.671 (2,1)	
			Open	472.891 (1,1)	1074.812 (1,2)	1558.326 (2,1)	
		0.05	0.1	Closed	220.847 (1,1)	315.254 (1,2)	501.467 (1,3)
				Open	223.686 (1,1)	319.359 (1,2)	508.376 (1,3)
0.2	Closed	212.326 (1,1)	302.865 (1,2)	481.042 (1,3)			
	Open	217.743 (1,1)	310.726 (1,2)	494.265 (1,3)			
0.1	0.1	Closed	432.688 (1,1)	612.130 (1,2)	958.963 (1,3)		
		Open	437.994 (1,1)	619.721 (1,2)	971.419 (1,3)		
0.2	Closed	414.362 (1,1)	584.804 (1,2)	912.223 (1,3)			
	Open	424.380 (1,1)	599.165 (1,2)	935.676 (1,3)			

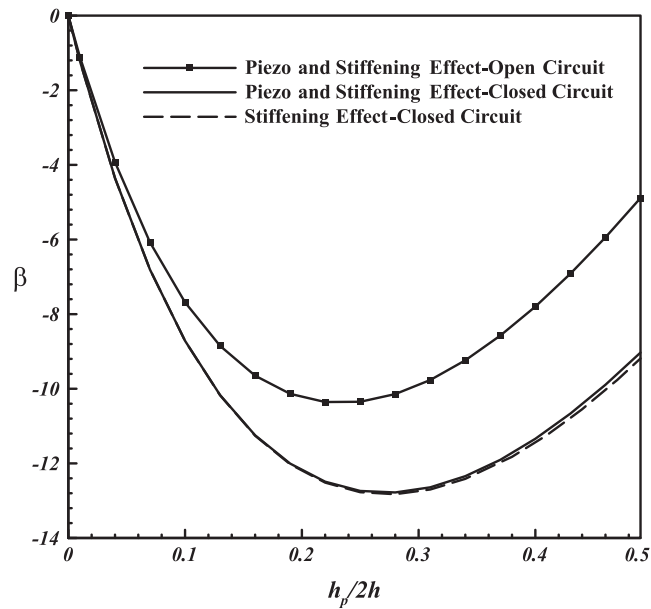


Fig. 3. The variation with the thickness ratio of parameter  $\beta$  for SFSF hybrid rectangular plate ( $b/a=1, 2h/a=0.05$ ) for closed and open circuit piezoelectric layers.

computed frequencies agree well with those of Ref. [28]. In Table 4, we have compared the resonant frequency of a homogeneous plate with the 3D analytical solution of Ref. [33]. Even for  $2h/a=1/12$ , the FSDT gives first five frequencies that agree well with those obtained when the problem is analyzed as 3D. We finally compare our results with those of He et al.

[30] who used the CLPT and the FEM to compute frequencies of a plate. Table 5 lists the first ten natural frequencies of a square isotropic plate with Ti-6Al-4V core, the top and the bottom G-1195 N piezoelectric layers,  $a=b=40$  cm,  $h=5$  mm, and  $h_p=0.1$  mm. It can be seen from values listed in Table 5 that frequencies predicted by the CLPT are a little lower (by at most 3.5%) instead of being a little higher than those given by the FSDT. It is possible that the FE mesh used in [30] did not give fully converged values of the frequencies.

#### 4.2. Frequencies of hybrid plates

We have listed in Table 6 the first three natural frequencies of hybrid plates of aspect ratio,  $b/a$ , equal to 1 and 2, thickness-length ratio ( $2h/a$ )=0.05 and 0.1, and  $h_p/2h=0.1$  and 0.2, open and closed circuit piezoelectric layers, and symmetric and asymmetric mechanical boundary conditions. These results imply that with the doubling of the plate width  $b$ , the natural frequency decreases for all types of mechanical boundary conditions except SFSF, and for both closed and open circuit electrical boundary conditions on major surfaces of the plate. Also doubling the value of  $2h/a$  enhances the natural frequency. For fixed electrical boundary conditions, natural frequencies monotonically increase as mechanical boundary conditions on edges  $y=b/2$  and  $y=-b/2$  are changed in the following sequence: SFSF, SSSF, SFSC, SSSS, SSSC and SCSC. Of course, mode shapes depend upon the boundary conditions.

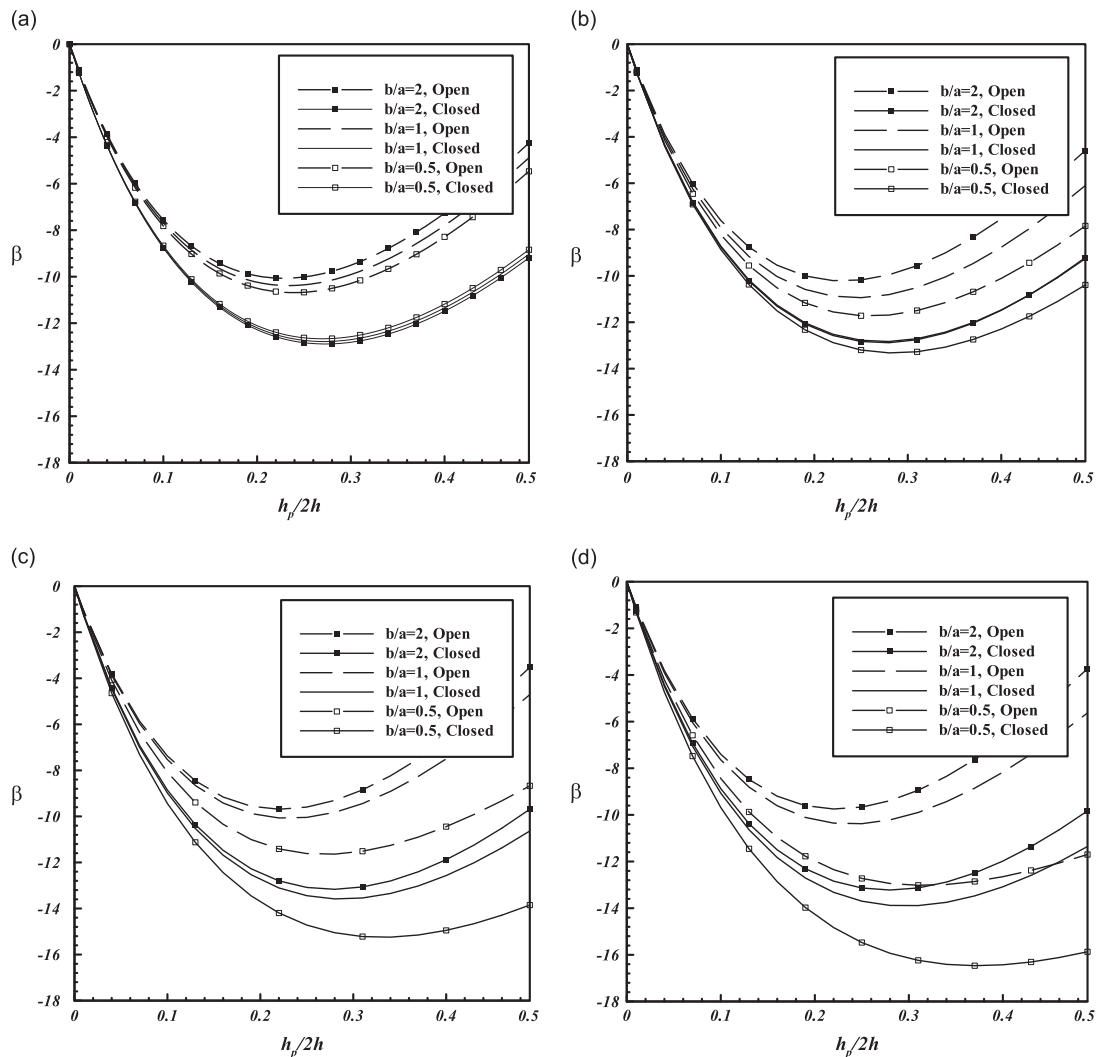


Fig. 4. For  $b/a=0.5, 1$  and  $2$ , variation with the thickness ratio of parameter  $\beta$  for hybrid: (a) SFSF, (b) SFSC, (c) SSSC, and (d) SCSC rectangular plates of aspect ratio ( $2h/a=0.05$ ) for closed and open circuit piezoelectric layers.

### 4.3. Effect of piezoelectric layer thickness

Fig. 3 shows the effect of the piezoelectric layer thickness on the fundamental frequency of a square SFSF hybrid rectangular plate with  $2h/a = 0.05$ . In order to quantify the effect of the piezoelectric layer thickness, we define the relative difference  $\beta$  in a natural frequency by

$$\beta = \frac{\omega|_{(\text{With piezoelectric layer})} - \omega|_{(\text{Without piezoelectric layer})}}{\omega|_{(\text{Without piezoelectric layer})}} \times 100 \quad (29)$$

For  $b/a = 1$ ,  $2h/a = 0.05$ , results exhibited in Fig. 3 reveal that for a fixed value of  $h_p/2h$  the magnitude of  $\beta$  is greater when boundary conditions on major surfaces of the piezoelectric layers are closed circuit than that when they are open circuit. Negative values of  $\beta$  imply that the hybrid plate has lower frequency than the corresponding core plate. For the closed circuit piezoelectric layers, the electro-mechanical coupling due to the matrix  $[e]$  has virtually no effect on the

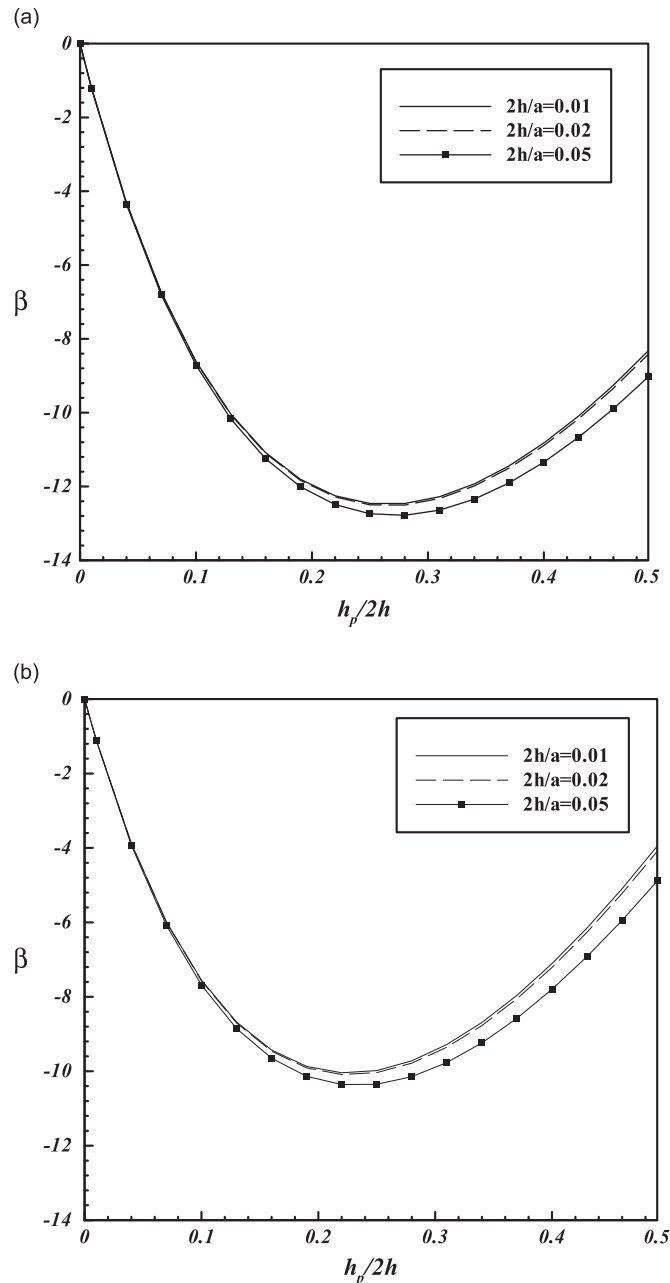
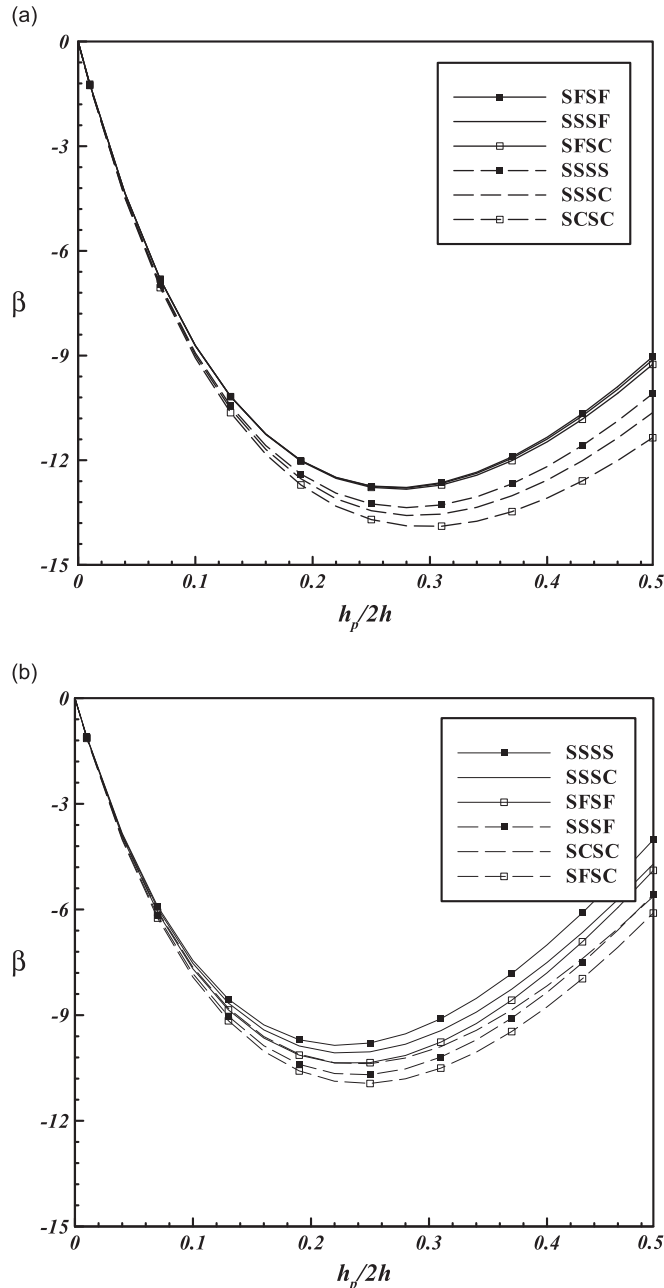
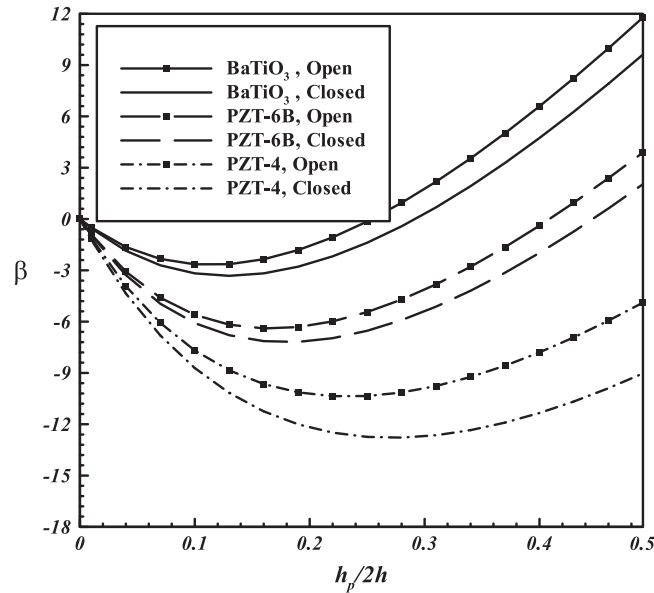


Fig. 5. The variation with the thickness ratio of parameter  $\beta$  for hybrid square plates under SFSF boundary condition: (a) closed circuit and (b) open circuit.

fundamental frequency. Since the mass density of the piezoelectric material is higher than that of material of the core, the mean density of the coupled structure increases with an increase in thickness ratio,  $h_p/2h$ . Values of the elastic moduli of the core material are higher than that of the piezoelectric material. These two effects tend to decrease the frequency of the hybrid plate as compared to that of the homogeneous non-piezoelectric material plate. However, the electromechanical coupling tends to increase the frequency. Initially the mass density and the stiffness effects exceed those due to electromechanical coupling. The electro-mechanical coupling effect increases with an increase in  $h_p/2h$  and should increase the value of  $\beta$ . Negative values of  $\beta$  for values of  $h_p/2h$  considered in this work suggest that the electro-mechanical coupling effect is less than that due to the combined effects of the increase in the mass density and the decrease in the stiffness. For a similar problem studied by Batra and Liang considering 3-D deformations, the value of  $\beta$  was found to be negative for the first five frequencies.



**Fig. 6.** The variation with the thickness ratio of parameter  $\beta$  for hybrid square plates ( $2h/a = 0.05$ ) under different boundary conditions: (a) closed circuit and (b) open circuit.



**Fig. 7.** For three piezoelectric materials, the variation with the thickness ratio of parameter  $\beta$  for hybrid square plates ( $2h/a = 0.05$ ) under SFSF boundary condition.

In Fig. 4, we have displayed effect of the thickness ratio on values of  $\beta$  for the first natural frequency in both closed and open circuit piezoelectric layers under different mechanical boundary conditions and three values, namely, 0.5, 1 and 2 of  $b/a$ . From results for the SFSF hybrid plate shown in Fig. 4(a), we conclude that for open circuit conditions, the magnitude of  $\beta$  decreases as  $b/a$  is increased from 0.5 to 2; however, for closed circuit conditions the ratio  $b/a$  has a converse effect on the magnitude of  $\beta$ . This effect is more noticeable for the open circuit condition than that for the closed circuit condition. For each set of boundary conditions, the magnitude of  $\beta$  first increases with an increase in  $h_p/2h$  and then decreases. The value of  $h_p/2h$  for which the magnitude of  $\beta$  is maximum depends upon boundary conditions on the edges  $y = -b/2, b/2$  and on the electric boundary conditions imposed on major surfaces of the piezoelectric layer. As should be clear from results depicted in Fig. 4(b), (c) and (d) for the SFSC, SSSC and SCSC plates, respectively, the magnitude of  $\beta$  is more for closed circuit boundary conditions than that for open circuit boundary conditions. Furthermore, the magnitude of  $\beta$  decreases as  $b/a$  increases from 0.5 to 2 for both open and closed circuit conditions.

For the first frequency of the SFSF hybrid plate having  $2h/a = 0.01, 0.02$  and  $0.05$ , we have plotted in Fig. 5 the variation of  $\beta$  with  $h_p/2h$  for both open and closed circuit boundary conditions. The magnitude of  $\beta$  increases with an increase in the value of  $2h/a$ . For each one of the three values of  $2h/a$ , the magnitude of  $\beta$  increases with an increase in the value of  $h_p/2h$  till  $h_p/2h = 0.28$  and  $0.25$  for closed and open circuit boundary conditions, respectively; subsequently, the magnitude of  $\beta$  decreases with an increase in the value of  $h_p/2h$ .

The effect of thickness ratio,  $h_p/2h$ , on  $\beta$  for different mechanical boundary conditions on the edges  $y = -b/2, b/2$  and for both closed and open circuit piezoelectric layers is depicted in Fig. 6(a) and (b), respectively. Results exhibited in Fig. 6(a) for closed circuit piezoelectric layers imply that the magnitude of  $\beta$  increases with the change in the boundary conditions on the edges  $y = -b/2, b/2$  in the following order: SFSF, SSSF, SFSC, SSSS, SSSC and SCSC. However, for the open circuit piezoelectric layers, this order of mechanical boundary conditions is SSSS, SSSC, SFSF, SSSF, SCSC and SFSC.

For the square SFSF hybrid plate with  $2h/a = 0.05$ , we have plotted in Fig. 7 the variation in  $\beta$  with  $h_p/2h$  for three materials of the piezoelectric layer and for both open and closed circuit boundary conditions. The magnitude of  $\beta$  for  $\text{BaTiO}_3$  is the least and that for  $\text{PZT-4}$  the most. The results for the three materials of the piezoelectric layers are qualitatively similar to each other but the value of  $h_p/2h$  for which the magnitude of  $\beta$  is the maximum is different.

#### 4.4. Effect of in-plane displacements

In order to investigate the effect of in-plane displacements on the plate natural frequencies, we solve the problem by setting  $u_0 = v_0 = 0$  in Eq. (1). Since there is no coupling between the stretching and the bending equations, requiring  $u_0 = v_0 = 0$  does not change values of the bending frequencies. The first ten natural frequencies for both closed and open circuit piezoelectric layers under different mechanical boundary conditions are listed in Table 7. It is seen that considering the in-plane displacements of the mid-surface includes frequencies of in-plane modes of vibrations among the first ten lowest frequencies. The absence of in-plane modes of vibration in Srinivas et al.'s [33] solution of the 3D problem was pointed out by Batra and Aimmanee [34].

**Table 7**

The effect of mid-plane displacement on the first ten natural frequencies (Hz) for both closed and open circuit piezoelectric layers under different mechanical boundary conditions ( $b/a=1$ ;  $2h/a=0.1$ ;  $h_p/2h=0.2$ ).

BCs	Electrical conditions	In-plane displacement	Mode sequences									
			1st	2nd	3th	4th	5th	6th	7th	8th	9th	10th
SSSS	Closed	With	778.28 (1,1)	1810.74 (1,2)	2727.76 (2,2)	3290.50 (1,3)	4077.56 (2,3)	5040.77 (1,4)	5269.30 (3,3)	5711.71 (2,4)	6751.17 (3,4)	6948.30 (1,5)
		Without	778.28 (1,1)	1810.74 (1,2)	2727.76 (2,2)	3290.50 (1,3)	4077.52 (2,3)	5040.77 (1,4)	5269.30 (3,3)	5711.71 (2,4)	6751.17 (3,4)	6948.30 (1,5)
	Open	With	802.01 (1,1)	1860.77 (1,2)	2797.50 (2,2)	3371.56 (1,3)	4172.06 (2,3)	5149.96 (1,4)	5381.12 (3,3)	5829.61 (2,4)	6880.72 (3,4)	7080.44 (1,5)
		Without	802.01 (1,1)	1860.77 (1,2)	2797.49 (2,2)	3371.56 (1,3)	4172.06 (2,3)	5149.96 (1,4)	5381.13 (3,3)	5829.61 (2,4)	6880.72 (3,4)	7080.44 (1,5)
SCSC	Closed	With	1068.63 (1,1)	1939.22 (2,1)	2299.91 (1,2)	3031.81 (2,2)	3350.00 (3,1)	3831.35 (1,3)	4233.91 (1,4)	4248.07 (3,2)	4466.29 (2,3)	4923.45 (1,5)
		Without	1068.63 (1,1)	1939.22 (2,1)	2299.91 (1,2)	3031.81 (2,2)	3350.00 (3,1)	3831.35 (1,3)	–	4248.07 (3,2)	4466.29 (2,3)	–
	Open	With	1097.01 (1,1)	1989.42 (2,1)	2351.26 (1,2)	3098.56 (2,2)	3429.51 (3,1)	3904.06 (1,3)	4233.91 (1,4)	4337.47 (3,2)	4550.40 (2,3)	4923.45 (1,5)
		Without	1097.01 (1,1)	1989.42 (2,1)	2351.26 (1,2)	3098.56 (2,2)	3429.51 (3,1)	3904.06 (1,3)	–	4337.47 (3,2)	4550.40 (2,3)	–
SFSF	Closed	With	387.51 (1,1)	620.53 (1,2)	1341.60 (1,3)	1453.44 (2,1)	1690.79 (2,2)	1791.51 (1,4)	2410.28 (2,3)	2567.56 (1,6)	2971.24 (3,1)	3170.16 (3,2)
		Without	387.51 (1,1)	620.53 (1,2)	1341.60 (1,3)	1453.44 (2,1)	1690.79 (2,2)	–	2410.28 (2,3)	–	2971.24 (3,1)	3170.16 (3,2)
	Open	With	395.67 (1,1)	625.84 (1,2)	1368.42 (1,3)	1485.17 (2,1)	1715.24 (2,2)	1791.51 (1,4)	2449.66 (2,3)	2567.56 (1,5)	3030.47 (3,1)	3218.32 (3,2)
		Without	395.67 (1,1)	625.84 (1,2)	1368.42 (1,3)	1485.17 (2,1)	1715.24 (2,2)	–	2449.66 (2,3)	–	3030.47 (3,1)	3218.32 (3,2)

## 5. Conclusions

We have used the first order shear deformation plate theory to study free vibrations of a transversely isotropic rectangular plate with surface bonded piezoelectric layers. Equations governing vibrations of the plate derived by using Hamilton's principle are uncoupled by introducing four auxiliary functions. The hybrid plate is simply supported on two opposite edges with the electric potential prescribed there enabling us to use a Levy type solution. The uncoupled ordinary differential equations are solved analytically. Numerical results included in the paper enable us to draw the following conclusions:

1. For a hybrid plate with identical piezoelectric layers perfectly bonded to the top and the bottom surfaces of the core plate, frequencies of transverse (bending) vibrations are independent of those for in-plane vibrations. Whereas frequencies of in-plane vibrations are the same for the open circuit and the closed circuit boundary conditions on major surfaces of the piezoelectric layers, those of transverse vibrations are different.
2. For all boundary conditions except SFSF, plate's fundamental natural frequency increases with an increase in plate's aspect ratio (length/width).
3. For the material systems considered, an increase in the piezoelectric layer thickness first decreases the fundamental natural frequency of the hybrid plate till the difference between the two frequencies reaches a maximum. This critical value of the piezoelectric layer thickness depends upon the material of the piezoelectric layer for a fixed material of the core.
4. For two opposite edges of a rectangular hybrid plate simply supported, boundary conditions on the other two edges increase the fundamental frequency in the following order: SFSF, SSSF, SFSC, SSSS, SSSC and SCSC for closed circuit piezoelectric layers, and SSSS, SSSC, SFSF, SSSF, SCSC and SFSC for open circuit piezoelectric layers.
5. For open circuit boundary conditions the change in the natural frequency is due to the stiffness effect as well as the piezoelectric effect, but for closed circuit boundary conditions it is due to the stiffness effect only. The three materials, namely, BaTiO<sub>3</sub>, PZT-6B and PZT-4, of the piezoelectric layer have qualitatively similar but quantitatively different effects on the fundamental frequency of the hybrid plate.

## Conflict of interest

None.

## Appendix A

The constitutive relation for a thin transversely isotropic piezoelectric material plate polarized in the  $z$ -direction can be written as

$$\begin{Bmatrix} \sigma_{xx} \\ \sigma_{yy} \\ \sigma_{xy} \\ \sigma_{xz} \\ \sigma_{yz} \end{Bmatrix} = \begin{bmatrix} \bar{c}_{11} & \bar{c}_{12} & 0 & 0 & 0 \\ \bar{c}_{12} & \bar{c}_{11} & 0 & 0 & 0 \\ 0 & 0 & \frac{1}{2}(\bar{c}_{11}-\bar{c}_{12}) & 0 & 0 \\ 0 & 0 & 0 & K^2 c_{55} & 0 \\ 0 & 0 & 0 & 0 & K^2 c_{55} \end{bmatrix} \begin{Bmatrix} \varepsilon_{xx} \\ \varepsilon_{yy} \\ \gamma_{xy} \\ \gamma_{xz} \\ \gamma_{yz} \end{Bmatrix} - \begin{bmatrix} 0 & 0 & \bar{e}_{31} \\ 0 & 0 & \bar{e}_{31} \\ 0 & 0 & 0 \\ -e_{15} & 0 & 0 \\ 0 & -e_{15} & 0 \end{bmatrix} \begin{Bmatrix} E_x \\ E_y \\ E_z \end{Bmatrix} \quad (\text{A.1.1})$$

$$\begin{Bmatrix} D_x \\ D_y \\ D_z \end{Bmatrix} = \begin{bmatrix} 0 & 0 & 0 & e_{15} & 0 \\ 0 & 0 & 0 & 0 & e_{15} \\ \bar{e}_{31} & \bar{e}_{31} & 0 & 0 & 0 \end{bmatrix} \begin{Bmatrix} \varepsilon_{xx} \\ \varepsilon_{yy} \\ \gamma_{xy} \\ \gamma_{xz} \\ \gamma_{yz} \end{Bmatrix} + \begin{bmatrix} \bar{\varepsilon}_{11} & 0 & 0 \\ 0 & \bar{\varepsilon}_{11} & 0 \\ 0 & 0 & \bar{\varepsilon}_{33} \end{bmatrix} \begin{Bmatrix} E_x \\ E_y \\ E_z \end{Bmatrix} \quad (\text{A.1.2})$$

where

$$\bar{c}_{11} = c_{11} - \frac{c_{13}^2}{c_{33}}, \quad \bar{c}_{12} = c_{12} - \frac{c_{13}^2}{c_{33}}, \quad \bar{e}_{31} = e_{31} - \frac{c_{13}}{c_{33}} e_{33}, \quad \bar{\varepsilon}_{33} = \varepsilon_{33} + \frac{e_{33}^2}{c_{33}} \quad (\text{A.1.3})$$

$K^2$  is the shear correction factor [26]

Coefficients in Eqs. (16) are defined as

$$(A'_{11}, A'_{12}) = \int_{-h}^h (Q_{11}, Q_{12}) dz + 2 \int_h^{h+h_p} (\bar{c}_{11}, \bar{c}_{12}) dz + \mu_7 \quad (\text{A.2.1})$$

$$A'_{55} = \int_{-h}^h Q_{55} dz + 2 \int_h^{h+h_p} c_{55} dz \quad (\text{A.2.2})$$

$$A'_{66} = \int_{-h}^h Q_{66} dz + \int_h^{h+h_p} (\bar{c}_{11} - \bar{c}_{12}) dz \quad (\text{A.2.3})$$

$$(D'_{11}, D'_{12}) = \int_{-h}^h (Q_{11}, Q_{12}) z^2 dz + 2 \int_h^{h+h_p} (\bar{c}_{11}, \bar{c}_{12}) z^2 dz + \mu_8 \quad (\text{A.2.4})$$

$$D'_{66} = \int_{-h}^h Q_{66} z^2 dz + \int_h^{h+h_p} (\bar{c}_{11} - \bar{c}_{12}) z^2 dz \quad (\text{A.2.5})$$

Coefficients in Eqs. (22) are given by

$$\lambda_1 = \mu_3 \lambda_3'' \lambda_1' + \mu_1 \lambda_3'' \lambda_1' + \mu_2 \lambda_1' + D'_{11} \lambda_1' \quad (\text{A.3.1})$$

$$\lambda_2 = \mu_3 \lambda_3'' \lambda_2' + \mu_1 \lambda_3'' \lambda_2' + \mu_3 \lambda_1'' + \mu_1 \lambda_1'' + \mu_2 \lambda_2' + D'_{11} \lambda_2' + I_2 \lambda_1' \omega_m^2 - K^2 A'_{55} \lambda_1' \quad (\text{A.3.2})$$

$$\lambda_3 = \mu_3 \lambda_3'' \lambda_3' + \mu_1 \lambda_3'' \lambda_3' + \mu_3 \lambda_2'' + \mu_2 \lambda_3' + \mu_1 \lambda_2'' + D'_{11} \lambda_3' + I_2 \lambda_2' \omega_m^2 - K^2 A'_{55} \lambda_2' - K^2 A'_{55} \quad (\text{A.3.3})$$

$$\lambda_4 = I_2 \lambda_3' \omega_m^2 - K^2 A'_{55} \lambda_3' \quad (\text{A.3.4})$$

$$\lambda_1' = \frac{S_2 \mu_3 \lambda_1''}{S_3} + \frac{S_2 \mu_1 \lambda_1''}{S_3} + \frac{S_1 \mu_3 \lambda_1''}{S_3} \quad (\text{A.3.5})$$

$$\lambda_2' = \frac{S_2 \mu_3 \lambda_2''}{S_3} + \frac{S_1 \mu_3 \lambda_2''}{S_3} + \frac{S_2 \mu_1 \lambda_2''}{S_3} - \frac{S_2 K^2 A'_{55}}{S_3} - \frac{S_1 K^2 A'_{55}}{S_3}, \quad \lambda_3' = -\frac{I_0 S_1 \omega_m^2}{S_3} \quad (\text{A.3.6-7})$$

$$\lambda_1'' = \frac{K^2 A'_{55}}{\mu_6} - \frac{\mu_4}{\mu_6}, \quad \lambda_2'' = \frac{I_0 \omega_m^2}{\mu_6}, \quad \lambda_3'' = \frac{K^2 A'_{55}}{\mu_6} - \frac{\mu_5}{\mu_6} \quad (\text{A.3.8-10})$$

where

$$\begin{aligned} \text{Closed - Circuit : } \mu_1 &= -\frac{4\bar{e}_{31}h_p}{3}, \quad \mu_2 = 0, \quad \mu_3 = \frac{8\bar{\epsilon}_{11}h_p}{9}, \quad \mu_4 = \frac{4e_{15}h_p}{3} \\ \text{Open - Circuit : } \mu_1 &= \frac{8\bar{e}_{31}(3h+h_p)}{3}, \quad \mu_2 = \frac{e_{15}\bar{e}_{31}h_p^2(h+h_p)}{\bar{\epsilon}_{33}}, \quad \mu_3 = \frac{16\bar{e}_{15}h_p}{3}, \quad \mu_4 = \frac{2e_{15}h_p}{\bar{\epsilon}_{11}} \\ \text{Closed - Circuit : } \mu_5 &= \frac{4h_p}{3}(\bar{e}_{31} + e_{15}), \quad \mu_6 = \frac{32\bar{\epsilon}_{33}}{3h_p}, \quad \mu_7 = 0, \quad \mu_8 = 0 \\ \text{Open - Circuit : } \mu_5 &= \frac{2e_{15}h_p}{\bar{\epsilon}_{11}} + \frac{2\bar{e}_{31}e_{15}h_p}{\bar{\epsilon}_{11}}, \quad \mu_6 = \frac{16e_{15}\bar{\epsilon}_{33}}{\bar{\epsilon}_{11}h_p}, \quad \mu_7 = \frac{2\bar{e}_{31}h_p}{\bar{\epsilon}_{33}}, \quad \mu_8 = \frac{\bar{e}_{31}^2 h_p(h+h_p)(2h+h_p)}{\bar{\epsilon}_{33}} \end{aligned} \quad (\text{A.3.11})$$

Furthermore,

$$S_1 = D'_{11} + \mu_1 \lambda_3'' + \mu_3 \lambda_3'' + \mu_2 \quad (\text{A.3.12})$$

$$S_2 = -\mu_3 \lambda_3'' - \mu_2 \quad (\text{A.3.13})$$

$$S_3 = S_2 I_2 + K^2 A'_{55} (S_1 + S_2) \quad (\text{A.3.14})$$

$$\eta_4 = \sqrt{\frac{\beta_j^2 A'_{33} - I_0 \omega_m^2}{A'_{11}}} \quad (\text{A.4.1})$$

$$\eta_5 = \sqrt{\frac{\beta_j^2 A'_{66} - I_0 \omega_m^2}{A'_{66}}} \quad (\text{A.4.2})$$

$$\eta_6 = \sqrt{\frac{\beta_j^2 D'_{66} + K^2 A'_{66} - I_2 \omega_m^2}{D'_{66}}} \quad (\text{A.4.3})$$

## References

- [1] H. Sumali, K. Meissner, H.H. Cudney, A piezoelectric array for sensing vibration modal coordinates, *Sensors and Actuators A* 93 (2001) 123–131.
- [2] T. Wu, Modeling and Design of a Novel Cooling Device for Microelectronics using Piezoelectric Resonating Beams, PhD Thesis Department of Mechanical and Aerospace Engineering, North Carolina State University, 2003.

- [3] F. Casadei, L. Dozio, M. Ruzzene, K.A. Cunefare, Periodic shunted arrays for the control of noise radiation in an enclosure, *Journal of Sound and Vibration* 329 (2010) 3632–3646.
- [4] D.H. Cortes, S.K. Datta, O.M. Mukdadi, Elastic guided wave propagation in a periodic array of multi-layered piezoelectric plates with finite cross-sections, *Ultrasonics* 50 (2010) 347–356.
- [5] Z. Hao, B. Liao, An analytical study on interfacial dissipation in piezoelectric rectangular block resonators with in-plane longitudinal-mode vibrations, *Sensors and Actuators A* 163 (2010) 401–409.
- [6] H.F. Tiersten, *Linear Piezoelectric Plate Vibrations*, Plenum, New York, 1969.
- [7] J. Wang, J. Yang, Higher-order theories of piezoelectric plates and applications, Reprinted from *Applied Mechanics Reviews* 53(4) (2000) 87–99.
- [8] R.C. Batra, S. Vidoli, Higher order piezoelectric plate theory derived from a three-dimensional variational principle, *AIAA Journal* 40 (1) (2002) 91–104.
- [9] H.S. Tzou, C.I. Tseng, Distributed piezoelectric sensor/actuator design for dynamic measurement/control of distributed parameter systems: a piezoelectric finite element approach, *Journal of Sound and Vibration* 138 (1) (1990) 17–34.
- [10] P. Heyliger, S. Brooks, Free vibration of piezoelectric laminates in cylindrical bending, *International Journal of Solids and Structures* 32 (20) (1995) 2945–2960.
- [11] R.C. Batra, X.Q. Liang, J.S. Yang, The vibration of simply supported rectangular elastic plate due to piezoelectric actuators, *International Journal of Solids and Structures* 33 (11) (1996) 1597–1618.
- [12] J.N. Reddy, On laminated composite plates with integrated sensors and actuators, *Engineering Structures* 21 (1999) 568–593.
- [13] S.S. Vel, R.C. Mewer, R.C. Batra, Analytical solution for the cylindrical bending vibration of piezoelectric composite plates, *International Journal of Solids and Structures* 41 (2004) 1625–1643.
- [14] B.P. Baillargeon, S.S. Vel, Exact solution for the vibration and active damping of composite plates with piezoelectric shear actuators, *Journal of Sound and Vibration* 282 (2005) 781–804.
- [15] G. Akhras, W.C. Li, Three-dimensional static, vibration and stability analysis of piezoelectric composite plates using a finite layer method, *Smart Material and Structures* 16 (2007) 561–569.
- [16] P. Topdar, A.H. Sheikh, N. Dhang, Vibration characteristics of composite/sandwich laminates with piezoelectric layers using a refined hybrid plate model, *International Journal of Mechanical Sciences* 49 (2007) 1193–1203.
- [17] M. Pietrzakowski, Piezoelectric control of composite plate vibration: effect of electric potential distribution, *Computers and Structures* 86 (2008) 948–954.
- [18] D.F. Torres, P.R. Mendonça, HSDT-layerwise analytical solution for rectangular piezoelectric laminated plates, *Composite Structures* 92 (2010) 1763–1774.
- [19] J. Jin, R.C. Batra, Effect of electromechanical coupling on static deformations and natural frequencies, *IEEE Transactions on Ultrasonics, Ferroelectrics, and Frequency Control* 52 (7) (2005) 1079–1093.
- [20] X.Q. Liang, R.C. Batra, Changes in frequencies of a laminated plate caused by embedded piezoelectric layers, *AIAA Journal* 35 (1997) 1672–1673.
- [21] C.L. Davis, G.A. Lesieutre, An actively tuned solid-state vibration absorber using capacitive shunting of piezoelectric stiffness, *Journal of Sound and Vibration* 232 (3) (2000) 601–617.
- [22] N. Wu, Q. Wang, S.T. Quek, Free vibration analysis of piezoelectric coupled circular plate, *Journal of Sound and Vibration* 329 (2010) 1126–1136.
- [23] W.H. Duan, S.T. Quek, Q. Wang, Free vibration analysis of piezoelectric coupled thin and thick annular plate, *Journal of Sound and Vibration* 281 (2005) 119–139.
- [24] P.R. Heyliger, Exact solutions for simply supported piezoelectric plates, *Journal of Applied Mechanics* 46(1997) 299–306.
- [25] D.A. Saravanos, P.R. Heyliger, D.A. Hopkins, Layerwise mechanics and finite element for the dynamic analysis of piezoelectric composite plates, *International Journal of Solids and Structures* 34 (1997) 359–378.
- [26] J.N. Reddy, *Energy and Variational Methods in Applied Mechanics*, John Wiley & Sons, New York, 1984.
- [27] Q. Wang, S.T. Quek, C.T. Sun, X. Liu, Analysis of piezoelectric coupled circular plate, *Smart Materials and Structures* 10 (2) (2001) 229.
- [28] Sh. Hosseini Hashemi, S.R. Atashipour, M. Fadaee, An exact analytical approach for in-plane and out-of-plane free vibration analysis of thick laminated transversely isotropic plates, *Archive of Applied Mechanics* 82 (5) (2012) 677–698.
- [29] A. Hasani Baferani, A.R. Saidi, H. Ehteshami, Accurate solution for free vibration analysis of functionally graded thick rectangular plates resting on elastic foundation, *Composite Structures* 93 (7) (2011) 1842–1853.
- [30] X.Q. He, T.Y. Ng, S. Sivashanker, K.M. Liew, Active control of FGM plates with integrated piezoelectric sensors and actuators, *International Journal of Solids and Structures* 38 (2001) 1641–1655.
- [31] A.W. Leissa, *Vibration of Plates*, NASA Report SP-160, Washington, DC, 1969.
- [32] A. Hasani Baferani, A.R. Saidi, E. Jomehzadeh, An exact solution for free vibration of thin functionally graded rectangular plates, *Proceedings of the Institution of Mechanical Engineers, Part C: Journal of Mechanical Engineering Science* 225 (3) (2011) 526–536.
- [33] S. Srinivas, C.V.J. Rao, A.K. Rao, An exact analysis for vibration of simply supported homogeneous and laminate thick rectangular plates, *Journal of Sound and Vibration* 12 (1970) 187–199.
- [34] R.C. Batra, S. Aimmanee, Missing frequencies in previous exact solutions of free vibrations of simply supported rectangular plates, *Journal of Sound and Vibration* 265 (2003) 887–896.
- [35] J.Y. Chen, H.L. Chen, E. Pan, P.R. Heyliger, Modal analysis of magneto-electro-elastic plates using the state-vector approach, *Journal of Sound and Vibration* 304 (2007) 722–734.
- [36] F. Ramirez, P.R. Heyliger, E. Pan, Free vibration response of two-dimensional magneto-electro-elastic laminated plates, *Journal of Sound and Vibration* 292 (2006) 626–644.
- [37] S. Kapuria, P. Kumari, Extended Kantorovich method for coupled piezoelectricity solution of piezolaminated plates showing edge effects, *Proceedings of the Royal Society A—Mathematical Physical and Engineering Sciences* 469 (2013) Article Number: 20120565.
- [38] S. Kapuria, J.K. Nath, Coupled global-local and zigzag-local laminate theories for dynamic analysis of piezoelectric laminated plates, *Journal of Sound and Vibration* 292 (2013) 306–325.
- [39] S.S. Vel, R.C. Batra, Three-dimensional analytical solution for hybrid multilayered piezoelectric plates, *Journal of Applied Mechanics* 67 (2000) 558–567.
- [40] R.C. Batra, X.Q. Liang, Finite dynamic deformations of smart structures, *Computational Mechanics* 20 (1987) 427–438.
- [41] R.C. Batra, T.S. Geng, Enhancement of the dynamic buckling load for a plate by using piezoceramic actuators, *Smart Materials and Structures* 10 (2001) 925–933.
- [42] S. Kapuria, P. Kumari, J.K. Nath, Efficient modeling of smart piezoelectric composite laminates: a review, *Acta Mechanica* 214 (2010) 31–48.
- [43] L. Ederly-Azulay, H. Abramovich, Piezolaminated plates—highly accurate solutions based on the extended Kantorovich method, *Composite Structures* 84 (2008) 241–247.
- [44] A. Benjeddou, New insights in piezoelectric free-vibrations using simplified modeling and analyses, *Smart Structures and Systems* 5 (2009) 591–612.
- [45] S.M. Shiyekar, T. Kant, An electromechanical higher order model for piezoelectric functionally graded plates, *International Journal of Mechanics and Materials in Design* 6 (2010) 163–174.
- [46] J.S. Yang, R.C. Batra, Free vibrations of a piezoelectric body, *Journal of Elasticity* 34 (1994) 239–254.
- [47] Chopra, Review of State-of-Art of Smart Structures and Integrated Systems, *AIAA Journal* 40 (2002) 2145–2187.
- [48] J.S. Yang and R.C. Batra, Free Vibrations of a Linear Thermopiezoelectric Body, *J. Thermal Stresses* 18 (1995) 247–262.